Synthesis and Physical Properties of Liquid-Crystalline Copolymers with Azobenzene Segments

Jui-Hsiang Liu,[1] Ching-Dong Hsieh[2]

[1]*Department of Chemical Engineering and Institute of Electro-optical Science and Engineering, National Cheng Kung University, Tainan 70101, Taiwan*
[2]*Department of Chemical Engineering, National Cheng Kung University, Tainan 70101, Taiwan*

Received 1 April 2005; accepted 5 June 2005
DOI 10.1002/app.22776
Published online 16 December 2005 in Wiley InterScience (www.interscience.wiley.com).

ABSTRACT: To investigate the effects of photoisomerizable azobenzene segments on the liquid-crystalline characteristics and thermal properties of polymers, a series of liquid-crystalline homopolymers and copolymers with azobenzene segments was synthesized. The azobenzene contents of the copolymers were estimated with elemental analysis. The photoisomerization of the azobenzene derivatives was studied with ultraviolet–visible (UV–vis) spectroscopy. The UV–vis absorption of the copolymers was found to be parallel with the content of the azobenzene segments. UV irradiation was found to cause a decrease in the copolymer transmittance around 355 nm due to the photoinduced isomerization from entgegen (E) to zusammen (Z). The phase-transition temperatures and molecular weights of the polymers were investigated with differential scanning calorimetry and gel permeation chromatography, respectively. The variation in the phase-transition temperature of the homopolymers before and after UV (365 nm) irradiation was investigated. The bended Z structure was found to disturb the order of the orientation of liquid crystals and to lower the phase-transition temperature. The appearance of the polymer film was changed from opaque to clear after sufficient UV irradiation. The image recording of the polymer films was achieved after UV irradiation through a mask with pictures. The stability and reliability of the Nematic-Isotropic phase transition of the homopolymers was evaluated with repeated cycles of 365-nm UV irradiation and heating at 130°C. After the recycle phase transition was repeated nine times, no significant decay in the response and transmittance could be found. © 2005 Wiley Periodicals, Inc. J Appl Polym Sci 99: 2443–2453, 2006

Key words: films; liquid-crystalline polymers (LCP); isomer/isomerization; UV-vis spectroscopy

INTRODUCTION

The photochemically driven control of the phase structures of liquid crystals has been widely studied in the field of optical devices, such as optical switches.[1–5] It is well known that azobenzene undergoes isomerization from trans to cis under UV light irradiation, whereas the cis form can return to the trans form either photochemically or thermally. Such a geometrical change can produce concomitant changes in the physical and chemical properties not only in the azobenzene itself but also in the microenvironments around it. Such photonic control has been mainly applied in a nematic phase by means of transmission, reflection, and light-scattering systems.[6–9] When azobenzene is embedded in a nematic liquid crystal, the two isomers produce different environments, which are characterized by the two different molecular shapes. Thus, optical information can be detected as changes in the optical properties, such as birefringence, before and after photoisomerization of the azobenzene molecules in liquid-crystal systems. It has also been shown that the trans–cis photoisomerization of a guest azobenzene compound without a chiral moiety caused a change in the cholesteric pitch of a host cholesteric liquid crystal.[10–11] Kurihara et al.[12,13] also studied the photochemical switching of a compensated nematic liquid crystal, which was prepared by the addition of a chiral azobenzene compound and a nonphotochromic chiral compound with an opposite twisting ability in a host liquid crystal. Recently, Ruslim and Ichimura[14,15] reported conformational effects on the photochemical change in the helical structure of the cholesteric phase by the photoisomerization of azobenzene compounds with chiral moieties at different positions.

A lot of photoisomerizable mesogenic molecules have been reported that change their shape on photoirradiation.[16–20] When irradiated, for example, with UV light, they show entgegen-zusammen (E–Z) or cis–trans isomerization. Photoisomerizable compounds can be used in liquid-crystal host mixtures as switchable materials or for changing the birefringence of the host mixture. Polymerizable liquid-crystal mix-

Correspondence to: J.-H. Liu (jhliu@mail.ncku.edu.tw).
Contract grant sponsor: National Science Council of the Republic of China (Taiwan); contract grant number: NSC 91-2216-E-006-034.

tures comprising photoisomerizable compounds can be used for the preparation of patterned anisotropic polymer films.[21–22] The photoisomerizable compounds and the liquid-crystal mixtures and polymer films prepared thereof can be used, for example, as optical elements, such as color filters or polarization beam splitters, in information storage devices, anisotropic membranes for the permeation of gases, or in photoswitching devices.

The terms *liquid-crystalline* or *mesogenic material* or *liquid-crystalline* or *mesogenic compounds* should denote materials or compounds comprising one or more rod-shaped, lath-shaped, or disk-shaped mesogenic groups, that is, groups with the ability to induce liquid-crystal phase behavior. Rod-shaped and lath-shaped mesogenic groups are especially preferred. The compounds or materials comprising mesogenic groups do not necessarily have to exhibit a liquid-crystal phase themselves. It is also possible that they show liquid-crystal phase behavior only in mixtures with other compounds or when the mesogenic compounds or materials or the mixtures thereof are polymerized.[23–25]

In our previous studies,[26–30] we synthesized a series of chiral dopants and chiral polymers and investigated their optical properties and applications on liquid-crystal cells and recording films. In this investigation, we aimed to provide new compounds, in particular, polymerizable and/or mesogenic compounds, which were suitable as photoisomerizable compounds and for other uses, were easy to synthesize in a large range of derivatives, and preferably showed broad liquid-crystalline phases with high clearing points. The thermal properties of the monomers and polymers synthesized in this investigation were all estimated. The photoisomerization of azobenzene segments in the polymers, variation of phase-transition temperature, ultraviolet–visible (UV–vis) spectra, stability and reliability of Nematic-Isotropic (N–I) phase transition, and time-resolved measurements of the photochemical N–I phase transition of polymers were investigated.

EXPERIMENTAL

Measurements

Fourier transform infrared (FTIR) spectra were recorded on a Jasco VALOR III (Tokyo) FTIR spectrophotometer. NMR spectra were obtained on a Bruker AMX-400 (Darmstadt, Germany) high-resolution NMR spectrometer. Optical rotations were measured at 30°C in dimethylformamide with a Jasco DIP-360 automatic digital polarimeter with readings to ±0.001°. Elemental analyses were conducted with a Heraeus CHN—O (Darmstadt, Germany) rapid elemental analyzer. Gel permeation chromatography (GPC) measurements were carried out at 40°C on a Hitachi L-4200 (Osaka, Japan) instrument equipped with TSK gel GMH and G2000H columns (Toyosoda Kasei, Japan) with tetrahydrofuran as an eluent. Thermal analysis of the azobenzene compounds and polymer dispersed liquid crystal (PDLC) films were performed by differential scanning calorimetry (PerkinElmer, Norwalk, CT) at a heating and cooling rate of 10 K/min in a nitrogen atmosphere. The liquid-crystal phases were investigated with an Olympus BH-2 (Osaka, Japan) polarized optical microscope equipped with Mettler hot stage (model FP-82; Schwerzenbach, Switzerland), and the temperature scanning rate was determined at a rate of 5 K/min. Scanning electron microscopy photographs were measured with a Jeol JSM-35 (Osaka, Japan) instrument, and atomic force microscopy pictures were recorded on a Digital Instruments Nanoscope III analyzer DI NS3a-2/MMAFM (New York).

Materials

The monomers used in this investigation were all synthesized as following. The products were all identified with spectrophotometers. The monomers in Table I were synthesized with similar steps as the processes discussed for the following sample compounds.

4-(6-Hydroxyhexyloxy) benzoic acid (1)

4-Hydroxybenzoic acid (16.57 g, 120 mmol) was dissolved in a mixture of EtOH (42 mL) and H_2O (18 mL). KOH (17.8 g. 317.8 mmol) and a catalytic amount of KI dissolved in EtOH (50 mL) was added dropwise to the solution. 1-Chloro-6-hexanol (22.5 g, 165 mmol) was then added, and the solution was heated to reflux for 24 h. The resulting mixture was poured into water and extracted with ethyl ether. The water-phase solution was acidified with HCl diluted with water until it was weakly acidic. The resulting precipitate was filtered and washed several times with water. The crude product was recrystallized from EtOH/H_2O (4/1; yield = 19.1 g, 67%, mp = 139–140°C).

FTIR (cm^{-1}): 3249 (OH); 1685 (C═O); 1287, 1251 (C—O—C). ^{1}H-NMR (DMSO-d_6, δ, ppm): 12.6 (s, 1H, —COOH), 7.9 (d, 2H Ar, ortho to —COOH), 7.0 (d, 2 H, Ar, meta to —COOH), 4.4 (s, 1H, OH), 4.0 (t, 2H, —CH_2OPh—), 3.4 (t, 2H, —CH_2—OH), 1.28–1.74 (m, 8H).

4-(Acryloyloxyhexyloxy) benzoic acid (2)

Compound **1** (7.15 g, 30 mmol), *N,N*-dimethylaniline (4 g, 33.0 mmol), and a catalytic amount of 2,6-di-*tert*-butyl-*p*-cresol was dissolved in distilled 1,4-dioxane (50 mL). The solution was cooled with an ice/salt bath, and then, acryloyl chloride (9 mL, 99.3 mmol)

TABLE I
Elemental Analysis (EA) of the Synthesized Monomers

Monomer	R_1	R_2	n	Formula[a]	EA	C (%)	H (%)	N (%)
M1	H	H	3	$C_{20}H_{20}O_6$ (356)	Calcd	67.34	5.61	—
					Found	67.32	5.71	
M2			6	$C_{23}H_{26}O_6$ (398)	Calcd	69.33	6.58	—
					Found	69.50	6.64	
M3			11	$C_{28}H_{36}O_6$ (468)	Calcd	71.77	7.74	—
					Found	71.63	7.73	
M4		Cl	6	$C_{23}H_{25}O_6Cl$ (432.9)	Calcd	63.75	5.82	—
					Found	63.68	5.87	
M5	OCH_3	H	6	$C_{24}H_{28}O_7$ (428.5)	Calcd	67.28	6.59	—
					Found	67.12	6.61	
M6		Cl	6	$C_{24}H_{27}O_7Cl$ (463.5)	Calcd	62.20	5.88	—
					Found	62.16	5.93	
M7	Cl	H	6	$C_{23}H_{25}O_6Cl$ (432.9)	Calcd	63.76	5.82	—
					Found	63.59	5.84	
M8		Cl	6	$C_{23}H_{24}O_6Cl_2$ (467.3)	Calcd	59.06	5.18	—
					Found	58.77	5.20	
M9[b]	—	—	3	$C_{19}H_{20}N_2O_4$ (340)	Calcd	67.05	5.89	8.23
					Found	66.74	5.99	8.20
M10[b]	—	—	6	$C_{22}H_{26}N_2O_4$ (382)	Calcd	69.09	6.85	7.32
					Found	68.25	6.91	7.30
M11[b]	—	—	11	$C_{27}H_{36}N_2O_4$ (452)	Calcd	71.65	7.96	6.19
					Found	71.49	7.97	6.12

[a] Weight-average molecular weights appear in parentheses.
[b] Diazo derivatives in Scheme 2.

dissolved in distilled 1,4-dioxane (20 mL) was added dropwise under vigorous stirring. After a 24 h reaction was completed at room temperature, the solution was poured into cold water, and the precipitate was filtered. The crude product was washed several times with water and recrystallized twice from EtOH (yield = 6.3 g, 69%, K 88°C N 92°C I).

FTIR (cm^{-1}): 2945, 2864 (CH_2); 1725 (C═O); 1604, 1291, 1246 (C—O—C); 1675 (C═C). ^{1}H-NMR ($CDCl_3$, δ, ppm): 12.5 (s, 1H, —COOH); 8.0 (d, 2H, Ar, ortho to —COOH); 7.0 (d, 2H, Ar, meta to —COOH); 5.8, 6.4, 6.1 (s, 3H, H_2C═CH—); 4.1 (t, 2H, —$COOCH_2$—); 4.0 (t, 2H, —CH_2OPh—); 0.94–1.28 (m, 8H, —CH_2—).

4-Methoxyphenyl-4′-(6-acryloyloxyhexyloxy) benzoate (M2)

Compound **2** (2.92 g, 10.0 mmol) and 4-methoxyphenol (1.86 g, 15 mmol) were dissolved in CH_2Cl_2 (40 mL) at 30°C. *N,N′*-dicyclo-hexylcarbodiimide (3.09 g, 15.0 mmol) and *N,N′*-dimethyl-aminopyridine (0.1 g. 0.82 mmol) were dissolved in CH_2Cl_2 (30 mL), and the mixture was then added to the former solution. The mixture was stirred for 2 days at 30°C. The resulting solution was filtered and washed with water, dried with $MgSO_4$, and evaporated. The crude product was purified by column chromatography with silica gel with ethyl acetate/*n*-hexane = 1/4 as the eluate, and it was recrystallized twice from EtOH (yield = 2.6 g, 65%).

FTIR (cm^{-1}): 2933, 2865 (CH_2); 1725 (C═O); 1635 (C═C). ^{1}H-NMR (acetone-d_6, δ, ppm): 8.1 (d, 2 aromatic H, ortho to —COOPh—); 7.1 (d, 2 aromatic H, meta to —OCH_3); 7.0 (d, 2 aromatic H, meta to —COOPh—); 6.9 (d, 2 aromatic H, ortho to —OCH_3); 6.3, 6.2, 5.9 (s, 3H, H_2C═CH—); 4.1 (t, 2H, —$COOCH_2$—); 4.0 (t, 2H, —CH_2OPh—); 1.26–1.42 (m, 8H, —CH_2—); 3.81(s, 3H, —OCH_3).

4-Methoxyphenyl-4′-(6-acryloyloxypropyloxy) benzoate (**M1**) and 4-methoxyphenyl-4′-(6-acryloyloxyundecyloxy) benzoate (**M3**) were synthesized with similar methods. The results of the elemental analysis and the thermal properties are summarized in Tables I and II, respectively.

4-Hydroxy-4′-methoxy-azobenzene (4)

p-Anisidine (10 g, 81.20 mmol) was dissolved in 1.5*M* aqueous HCl (100 mL) and kept in an ice bath at 0°C. Sodium nitrite (6 g, 86.96 mmol) in water (20 mL) was added dropwise to the former solution and stirred for 1 h. Sodium hydroxide (8.4 g, 0.21 mol) and phenol (8.4 g, 89.26 mmol) were dissolved in water (80 mL) and stirred at −2°C. The former solution was added dropwise to the latter solution at −2°C and then stirred for 1 h. The resulting mixture was poured into water, and the solution was acidized with 2*M* aqueous HCl to pH = 2. The crude product was washed with water twice until it was neutral, and it was recrystal-

TABLE II
Thermal Properties of the Monomers

Monomer	Mesophase (°C) and enthalpy (J/g)[a]		T_d (°C)
	Phase transitions for the heating cycle	Phase transitions for the cooling cycle	
M1	K 59 N 76 I 59.7, 2.39	K 2 I −30.8	322
M2	K 39 N 63 I 7.36, 91.3	K 28 N 44 I −84.6, −1.18	358
M3	K 61 I 126	K 17 S 39 N 51 I −30.7, −1.16, −1.41	459
M4	K 78 N 104 I 0.40, 0.32	K 12 N 75 I −0.63, −0.53	362
M5	K 77 I 95.0	—[b]	392
M6	K 64 I 92.6	—	357
M7	K 90 N 100 I 49.0, 1.73	K 22 I −39.0	445
M8	K 69 I 85.2	—	347
M9[c]	K 62 N 81 I —	K 38 N 48 I −0.98	300
M10[c]	K 85 I —	K 70 I —	304
M11[c]	K 66 N 70 I —	K 54 S 60 N 66 I —	310

T_d, decomposition temperature; K, crystal; S, smectic; N, nematic; I, isotropic.
[a] Enthalpy of the phase change during heating and cooling.
[b] Was not clearly obtained
[c] Azo derivatives in Scheme 2.

lized from EtOH (yield = 14.74 g, 80%, yellow crystalline powder).

FTIR (KBr, cm^{-1}): 3419 (OH). ^{1}H-NMR ($CDCl_3$, δ, ppm): 6.92–7.88 (m, 8H, aromatic); 3.9 (s, 3H, $ArOCH_3$).

1-Hydroxy-3-(4-methoxy-azobenzene-4′oxy)propane (5a)

Compound **4** (4.0 g, 17.52 mmol) was dissolved in EtOH (200 mL). KOH (1.12 g, 19.96 mmol) and a trace of KI dissolved in 30 mL of water were added dropwise to the former solution; 1-chloro-3-propanol (1.82 g, 19.25 mmol) dissolved in EtOH (20 mL) was then added. The solution was refluxed at 90°C for 24 h. The resulting mixture was poured into water and extracted with diethyl ether. The water phase was collected and acidized to pH = 2 and then washed with neutral water until it was neutral. The crude product was filtered and recrystallized from EtOH (yield = 4.06 g, 81%, yellow crystalline powder).

FTIR (KBr, cm^{-1}): 3280 (OH); 2948, 2872 (CH_2). ^{1}H-NMR ($CDCl_3$, δ, ppm): 6.99–7.89 (m, 8H, aromatic), 4.19–4.22 (t, 2H, OCH_2), 3.9 (s, 3H, $ArOCH_3$), 3.8–3.89 (t, 2H, OCH_2), 2.07–2.10 (m, 2H, $CH_2CH_2CH_2$).

TABLE III
Results of Homopolymerization[a]

Polymer[b]	Yield (%)	$M_w \times 10^{4c}$	$M_n \times 10^{4c}$	$M_z \times 10^{4c}$	PDI[d]
P-1	61	1.7	1.0	2.6	1.7
P-2	70	3.5	2.8	4.7	1.2
P-3	95	5.5	6.4	5.6	1.0
P-4	78	3.3	2.8	4.1	1.2
P-5	66	3.1	2.6	3.8	1.2
P-6	74	3.2	2.7	3.9	1.2
P-7	75	4.0	3.0	6.6	1.3
P-8	79	3.2	2.7	3.9	1.2
P-9	50	0.5	0.4	0.7	1.3
P-10	45	1.4	0.8	2.3	1.8
P-11	62	2.7	2.4	3.1	1.1

M_w, weight-average molecular weight; M_n, number-average molecular weight; M_z, z-average molecular weight; PDI, polydispersity index (M_w/M_n).
[a] In benzene at 60°C for 24 h in the presence of 3 mol % AIBN.
[b] Homopolymers of the monomers in Table I.
[c] Measured by GPC with a polystyrene standard.

1-Hydroxy-6-(4-methoxy-azobenzene-4′oxy)hexane (5b)

Compound **5b** was similarly synthesized as **5a** (yield = 66%, yellow crystalline powder).

TABLE IV
Thermal Properties of the Homopolymers

Polymer	Mesophase (°C) and enthalpy (J/g)[a]		T_d (°C)
	Phase transitions for the heating cycle	Phase transitions for the cooling cycle	
P-1	G 75 I 7.59	G 63 I 10.0	419
P-2	G 24 S 90 N 117 I 0.33, 2.15, 1.74	G 20 S 87 N 114 I 0.37, −2.55, −1.88	441
P-3	G 21 N 125 I 2.44, 9.34	G 20 N 114 I 0.94, −7.77	464
P-4	G 22 N 52 I 0.41, 1.42	G 17 N 48 I 0.33, −1.61	429
P-5	G 33 I 0.505	G 29 I 0.21	429
P-6	G 35 I 0.52	G 30 I 0.59	353
P-7	G 27 N 59 I 0.47, 0.38	G 21 N 55 I 0.33, −0.34	434
P-8	G 27 N 59 I 0.45, 0.41	G 25 N 56 I 0.35, −0.56	434
P-9[b]	G 47 N 98 I 0.38, 0.33	G 40 N 94 I 0.24, −0.44	376
P-10[b]	G 67 S 95 N 136 I 0.59, 3.87, 1.24	G 64 S 93 N 134 I 0.47, −3.55, −1.1	383
P-11[b]	G 69 S 123 I 18.1, 0.65	G 69 S 114 I 15.4, 0.84	330

T_d, decomposition temperature; K, crystal; S, smectic; N, nematic; I, isotropic.
[a] Enthalpy of the phase change during heating and cooling.
[b] Homopolymers of the azo derivatives in Scheme 2.

TABLE V
Results of Copolymerization[a]

Polymer	n	R_1	R_2	Yield (%)	$x:y$[b]	$M_w \times 10^4$[c]	$M_z \times 10^4$[c]	PDI
CoP-1	3	H	H	52	90/10	2.1	3.0	1.81
CoP-2	6			81	93/7	2.1	3.1	1.84
CoP-3	11			52	94/6	2.0	3.1	1.83
CoP-4	3	OCH_3	Cl	74	93/7	1.4	2.3	1.97
CoP-5	6			32	92/8	1.5	2.5	1.88
CoP-6	11			61	94/6	1.4	2.3	1.95
CoP-7	3	Cl		73	90/10	1.6	2.6	1.90
CoP-8	6			69	90/10	1.6	2.6	1.87
CoP-9	11			71	92/8	1.8	2.8	1.81

M_w, weight-average molecular weight; M_z, z-average molecular weight; PDI, polydispersity index (M_w/number-average molecular weight).
[a] In benzene at 60°C for 24 h in the presence of 3 mol % AIBN (initiator).
[b] Polymer composition calculated from elemental analysis.
[c] Measured by GPC with a polystyrene standard.

FTIR (KBr, cm^{-1}): 3300 (OH); 2938, 2864 (CH_2). ^{1}H-NMR (acetone-d_6, δ, ppm): 7.06–7.87 (m, 8H, aromatic), 4.08–4.11 (t, 2H, OCH_2), 3.89 (s, 3H, $ArOCH_3$), 3.52–3.55 (t, 2H, OCH_2), 1.44–1.83 [m, 8H, $CH_2(CH_2)_4CH_2$].

1-Hydroxy-11-(4-methoxy-azobenzene-4′oxy)undecane (5c)

Compound **5c** was similarly synthesized as **5a** (yield = 71%, yellow crystalline powder).

TABLE VI
Thermal Properties of the Copolymers

	Mesophase (°C) and enthalpy (J/g)[a]		
Polymer	Phase transitions for the heating cycle	Phase transitions for the cooling cycle	T_d (°C)
CoP-1	G 27 S 89 N 117 I 0.46, 1.91, 1.27	G 24 S 87 N 115 I 0.75, −1.66, −1.16	402
CoP-2	G 26 S 88 N 117 I 0.44, 2.06, 1.02	G 23 S 86 N 115 I 0.73, −1.92, −0.88	418
CoP-3	G 23 S 87 N 114 I 0.41, 1.55, 1.10	G 17 S 84 N 111 I 0.53, −1.51, −1.20	424
CoP-4	G 29 I 0.46	G 27 I 0.40	400
CoP-5	G 13 I 0.38	G 21 I 0.44	402
CoP-6	G 24 I 0.43	G 23 I 0.43	404
CoP-7	G 17 I 0.55	G 17 I 0.31	400
CoP-8	G 18 I 0.49	G 17 I 0.30	400
CoP-9	G 18 I 0.47	G 15 I 0.27	405

T_d, decomposition temperature; G, glassy state; S, smectic; N, nematic; I, isotropic.
[a] Enthalpy of the phase change during heating and cooling.

FTIR (KBr, cm^{-1}): 3301 (OH); 2917, 2849 (CH_2). ^{1}H-NMR (acetone-d_6, δ, ppm): 7.06–7.87 (m, 8H, aromatic), 4.07–4.11 (t, 2H, OCH_2), 3.88 (s, 3H, $ArOCH_3$), 3.47–3.51 (t, 2H, OCH_2), 1.24–1.82 [m, 18H, $CH_2(CH_2)_9CH_2$].

3-(4-Methoxy-4′-oxy-azobenzene)propyl acrylate (M9)

Compound **5a** (5.23 g, 18.3 mmol), *N,N*-dimethylaniline (2.98 g, 24.6 mmol), and a catalytic amount of 2,6-di-*tert*-butyl-*p*-cresol were dissolved in distilled 1,4-dioxane (30 mL). The solution was cooled in an ice bath, and then, acryloyl chloride (2 mL, 24.6 mmol) dissolved in distilled dioxane (30 mL) was added dropwise under vigorous stirring for 2 h. The mixture was stirred for 24 h at 55°C. After the reaction was completed, the solution was poured into ice water and recrystallized twice from EtOH (yield = 2.18 g, 53%, yellow crystalline powder).

FTIR (KBr, cm^{-1}): 2931, 2879, 2838 (CH_2); 1728 (C═O); 1635 (C═C). ^{1}H-NMR ($CDCl_3$, δ, ppm): 6.98–

TABLE VII
UV–Vis Optical Properties of the Copolymers

Sample	λ_{max} (nm)	ε_{max} ($\times 10^{-4}/cm^{-1}\ M^{-1}$)
CoP-1	262, 358	2.17, 1.98
CoP-2	262, 358	2.17, 2.02
CoP-3	262, 358	2.17, 2.02
CoP-4	270, 358	1.52, 1.98
CoP-5	270, 358	1.52, 2.02
CoP-6	270, 358	1.52, 2.02
CoP-7	270, 358	2.02, 1.95
CoP-8	270, 358	2.02, 2.02
CoP-9	270, 358	2.03, 2.02

ε_{max}, absorption coefficient calculated by Beer's law. λ_{max}, maximum absorbance wavelength.

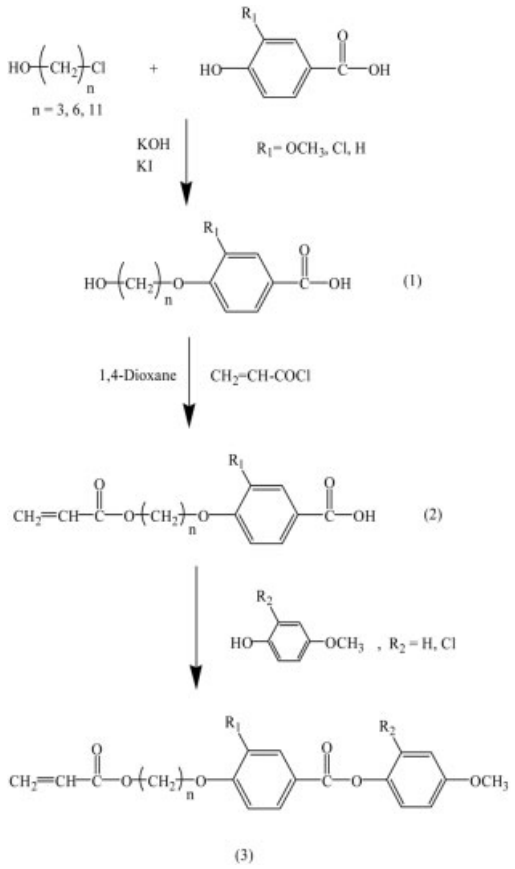

Scheme 1

7.89 (m, 8H, aromatic); 6.39–6.45, 5.82–5.86 (d, 2H, CH_2═CH); 6.09–6.18 (m, 1H, CH_2═CH); 4.36–4.40 (t, 2H, OCH_2); 4.12–4.16 (t, 2H, OCH_2); 3.88 (s, 3H, $ArOCH_3$); 2.16–2.24 (m, 2H, $CH_2CH_2CH_2$).

6-(4-Methoxy-4′-oxy-azobenzene)hexyl acrylate (m10)

Compound **M10** was similarly synthesized as **M9** (yield = 86%, yellow crystalline powder).

FTIR (KBr, cm^{-1}): 2940, 2863 (CH_2); 1716 (—C═O); 1631 (C═C). ^{1}H-NMR ($CDCl_3$, δ, ppm): 6.97–7.88 (m, 8H, aromatic); 6.38–6.43, 5.80–5.83 (d, 2H, CH_2═CH); 6.09–6.16 (m, 1H, CH_2═CH); 4.16–4.20 (t, 2H, OCH_2); 4.02–4.05 (t, 2H, OCH_2); 3.88 (s, 3H, $ArOCH_3$); 1.47–1.85 [m, 8H, $CH_2(CH_2)_4CH_2$].

11-(4-Methoxy-4′-oxy-azobenzene)undecyl acrylate (M11)

Compound **5c** was similarly synthesized as **M9** (yield = 88%, yellow crystalline powder).

FTIR (KBr, cm^{-1}): 2920, 2850 (CH_2); 1722 (C═O); 1637 (C═C). ^{1}H-NMR (acetone-d_6, δ, ppm): 7.05–7.87 (m, 8H, aromatic); 6.29–6.35, 5.83–5.87 (d, 2H, CH_2═CH); 6.08–6.17 (m, 1H, CH_2═CH); 4.07–4.13 (m, 4H, OCH_2); 3.88 (s, 3H, $ArOCH_3$); 1.32–1.85 [m, 18H, $CH_2(CH_2)_9CH_2$].

The results of the elemental analysis and the thermal properties of the monomeric diazo derivatives are also summarized in Tables I and II, respectively.

Polymerization

The homopolymers and copolymers were prepared by radical polymerization in a sealed ampule with 3 mol % azobisisobutyronitrile (AIBN) in anhydrous benzene at 60°C for 24 h. The polymer was purified by repeated precipitation with methanol and dried *in vacuo*. The results and the physical properties of the homopolymers and copolymers are shown in Tables III–VI. The compositions of the copolymers were estimated from the results of the elemental analysis.

Fabrication of the polymer cell

The polymer, dissolved in benzene, was cast on a glass plate. After drying, another glass was used to cover the surface of the polymer film. The surroundings of the cell were sealed with adhesive. The cell was heated to isotropic temperature and then cooled to room temperature. The thickness of the film was 25 μm.

RESULTS AND DISCUSSION

To investigate the effects of the photoisomerizable azobenzene segments on the liquid-crystalline charac-

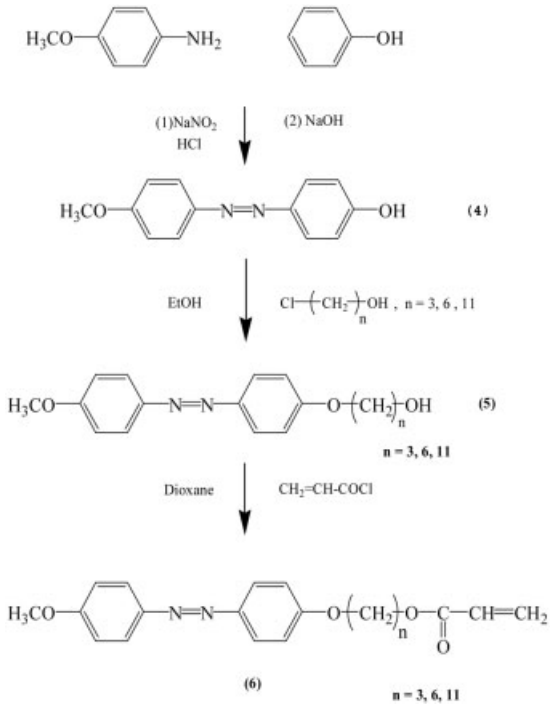

Scheme 2

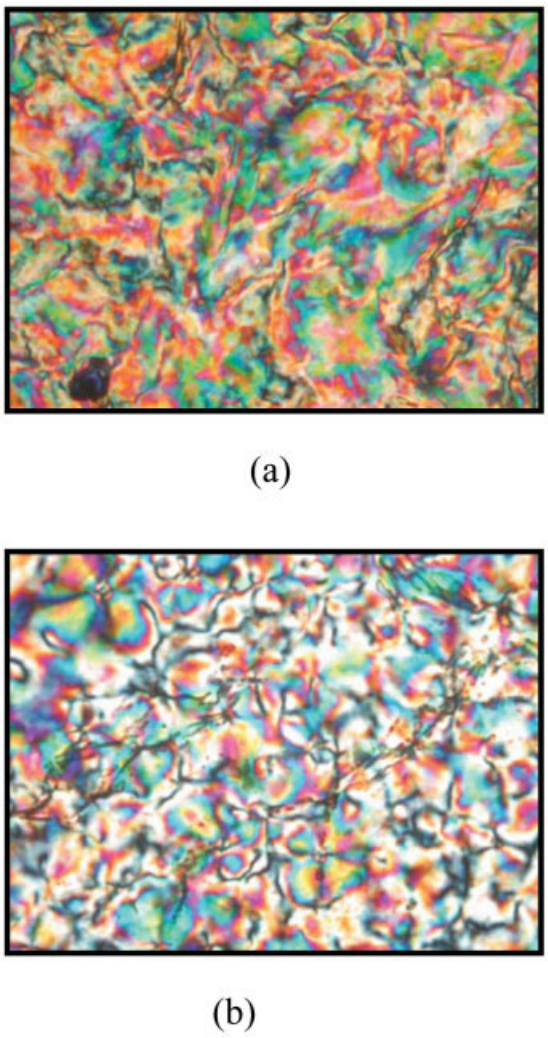

Figure 1 POM textures of monomers (a) **M2** and (b) **M4.**

teristics and thermal properties of the polymers, a series of homopolymers and copolymers with azobenzene segments were synthesized. The synthetic process of acrylates and azobenzene monomers with various methylene lengths and benzene-ring-attached groups are shown in Schemes 1 and 2, respectively. The results of the syntheses and the thermal properties of the monomers are summarized in Tables I and II.

Table I shows the results of the elemental analysis of the monomers. The molecular structures were also confirmed with NMR and FTIR spectroscopy. As shown in Table II, for acrylates, the methylene was too long, and the existence of a methoxy group at the R_1 position seemed to be unfavorable for the formation of liquid-crystalline phases. Azobenzene monomers with a N═N central part and balanced with terminal methoxy and alkyl acrylates showed liquid-crystalline phases. This may have been due to the insufficient molecular polarity at the central part and terminals; monomer **M10** with hexyl acrylate revealed no liquid-crystalline phases. In principle, reasonable central and terminal polarities are the basic requirements for liquid crystals. Polarities that are too strong or extremely weak usually give no proper intermolecular forces, which leads to the destruction of liquid-crystalline orientation. The phase-transition temperatures of the monomers were estimated with differential scanning calorimetry, and the liquid-crystalline phases were confirmed with a polarizing optical microscopy (POM) analyzer. Figure 1 shows some examples of the liquid-crystalline optical textures of the compounds. The liquid-crystalline phases were analyzed with a POM analyzer and then determined by a comparison of the optical textures of the compounds with those described in the literature. The liquid-crystalline phases were also identified with a small-angle X-ray diffraction analyzer. Figure 1 shows the POM textures of monomers **M2** and **M4.** The decomposition temperatures of the monomers were evaluated with a thermogravimetric analyzer and are summarized in Table II. As shown in Table II, all of the decomposition temperatures were higher than 300°C.

Table III shows the results of the homopolymerization of the monomers. For purification, the precipitated polymers were dissolved in solvent and then reprecipitated from methanol three times. The molecular weight of the polymers was estimated with a GPC analyzer with polystyrene as a standard. The molecular weight and polydispersity index of the polymers were estimated with a GPC-equipped data processor. The polymers revealed excellent film-forming properties. The thermal properties of the homopolymers are summarized in Table IV. Compared with the liquid-crystalline phases in Table II, the polymerization of the monomers seemed to balance the net polarity of the units leading to the existence of the liquid-crystal-

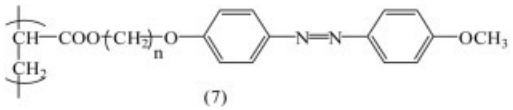

(7)

Homopolymers

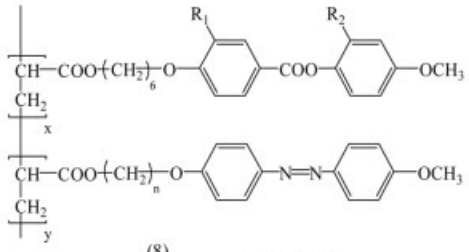

(8)

R_1= OCH_3, Cl

R_2= H, Cl

Copolymers

Scheme 3

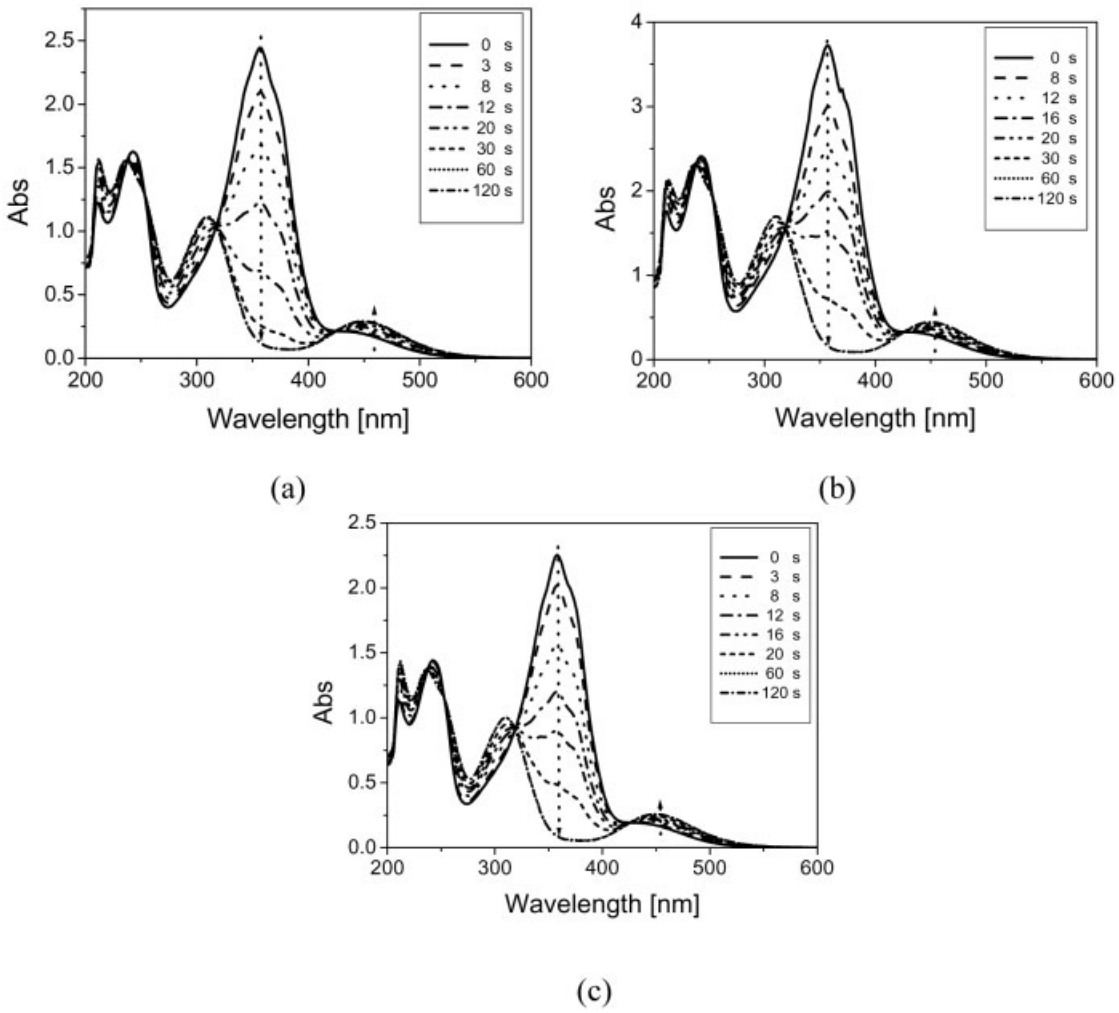

Figure 2 Variation of the UV–vis spectra of homopolymers (a) **P-9,** (b) **P-10,** and (c) **P-11** during UV irradiation.

line phases of **P-3** and **P-8.** The azobenzene-derived polymer **P-10** showed similar variations. After polymerization, mesogenic smectic and nematic phases were obtained. In general, the existence of stronger intermolecular forces at the central and terminal parts of molecules was favorable for the smectic and nematic phases, respectively.

Scheme 3 shows the structures of the homopolymers and copolymers. The results of the copolymerization and the feed comonomer compositions are summarized in Table V. The compositions of the copolymers were estimated with elemental analysis. The thermal properties of the copolymers are summarized in Table VI. Unlike in the homopolymers, the existence of the high electronegative chlorine at the R_2 position might have affected the polarity of the azobenzene segments, which led to the destruction of molecular interactions. The results suggest that a proper strength of molecular interaction was needed for the formation of the liquid-crystalline orientation. In addition to the high value of electronegativity, the volume of chlorine was relatively higher. The existence of a methoxy group at the R_1 position may have increased the extranegative direction of steric factors for the formation

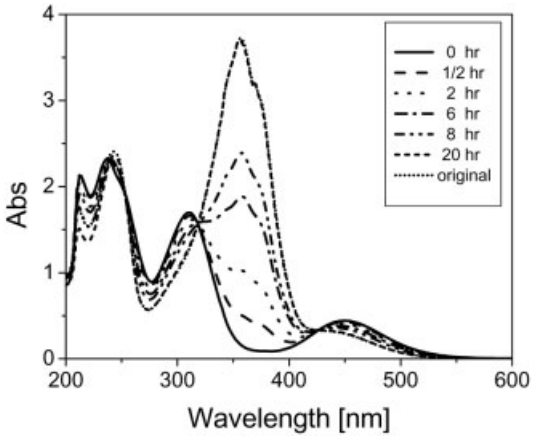

Figure 3 Stability of the UV–vis spectra of **P-10** in the dark.

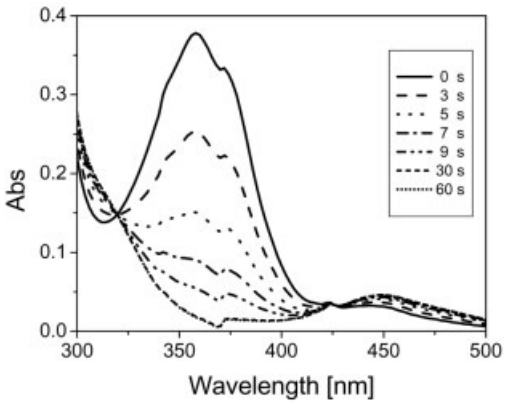

(a)

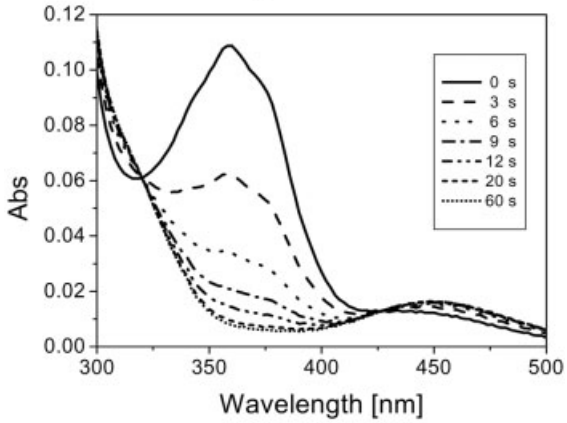

(b)

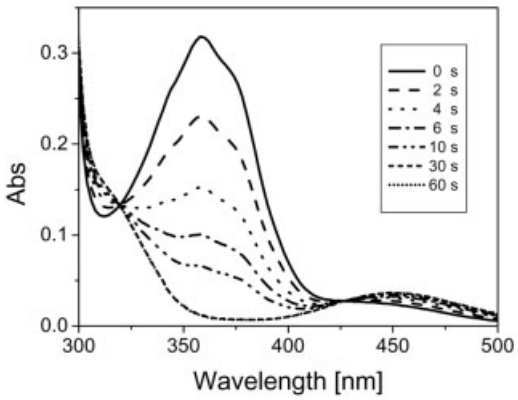

(c)

Figure 4 Variation of UV–vis spectra of copolymers (a) **CoP-1,** (b) **CoP-2,** and (c) **CoP-8** during UV irradiation.

of the liquid-crystalline phases. As shown in Table VI, the decomposition temperatures of the copolymers were all higher than 400°C.

Figure 2 shows the variation of the UV–vis spectra of the homopolymers **P-9, P-10,** and **P-11** during the period of UV irradiation. As shown in Figures 1 and 2,

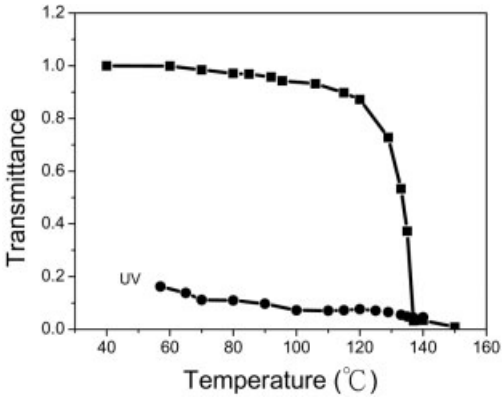

Figure 5 Variation in the phase-transition temperature of **P-10** (a, ■) before and (b, ●) after UV (365 nm) irradiation.

the main wavelength around 355 nm decreased with increasing UV irradiation. However, the absorption around 460 nm increased with increasing UV irradiation time. The variation of the absorptions may have been due to the geometric change from E to Z of the diazobenzene derivatives during UV irradiation. The absorption stability of the homopolymer **P-10** in dark surroundings is shown in Figure 3. As shown in Figure 3, the thermal stability of the **P-10** was around 20 h. The results show that the geometric Z form may have returned to the E form gradually, even without exposure to any UV light.

Furthermore, similar UV–vis spectra of copolymers are also shown in Figure 4. As shown in Table V, the diazobenzene content in the polymers was lower than 10%. Accordingly, the absorption level shown in Figure 4 was approximate to the unit contents in the copolymers. The decreasing tendency of the absorption of the UV irradiation was similar to those obtained in the homopolymer system shown in Figure 3.

The variation of the phase-transition temperature of the homopolymer **P-10** before and after UV (365 nm) irradiation is shown in Figure 5. The square and circular symbols denote the original phase-transition temperature from nematic to isotropic and the temperature after UV irradiation, respectively. The results suggest that the phase-transition temperature was shifted to a lower level. UV irradiation may have

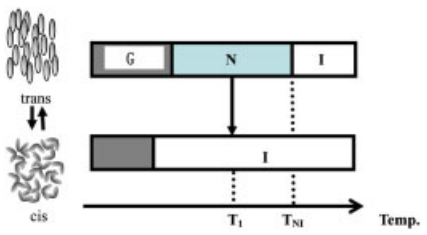

Figure 6 Variation in the phase-transition temperature on the photoisomerization of azobenzene polymers.

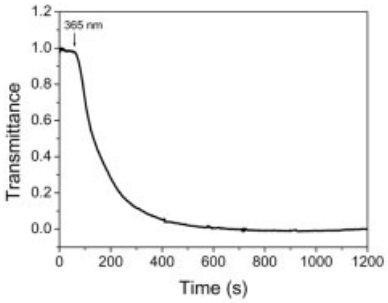

(a)

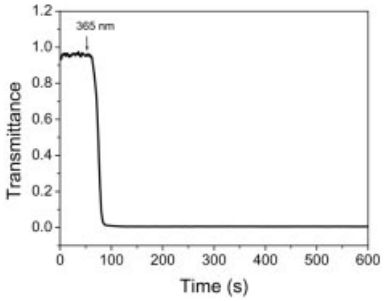

(b)

Figure 7 Time-resolved measurements of the photochemical N–I phase transition of **P-10** induced by UV (365 nm) irradiation at (a) 57 and (b) 110°C (glass-transition temperature = 67°C, $T_{N–I}$ = 136°C).

caused the E–Z photoisomerization of the azobenzene units. The bended Z structure may have disturbed the order of the orientation of the liquid crystals and lowered the phase-transition temperature. As shown in Figure 6, the disordering may have caused the decrease in the phase-transition temperature. The results suggest that at T_1 (any temperature in the Nematic phase) temperature, the appearance of the polymer film changed from opaque to clear after sufficient UV irradiation.

To investigate the dependence of the UV response on the temperature, time-resolved measurements of

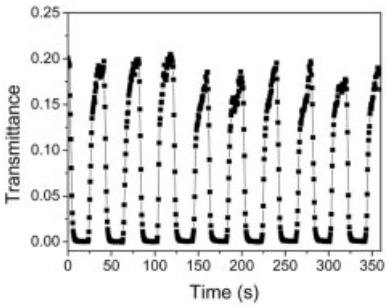

Figure 8 Stability and reliability of the N–I phase transition of **P-10;** the polymer was repeatedly irradiated with 365 nm of UV rays and then heated at 130°C.

Figure 9 Image recording of **P-10** by UV irradiation through masks; a black background was set behind the polymer film.

the photochemical N–I phase transition of homopolymer **P-10** were estimated at 57 and 110°C before and after UV irradiation. The glass transition and the N–I phase-transition temperatures of the **P-10** were 67 and 136°C, respectively. As shown in Figure 7(a,b), the variation of the transmittance revealed the phase transition from the nematic to the isotropic phase. If the film was irradiated at a temperature lower than the glass-transition temperature, the glassy state had to be conquered and then further disturbed to the isotropic phase. At temperatures near $T_{N–I}$ (the temperature from nematic to isotropic), the UV-induced bended azobenzene molecules may have disturbed the order of the orientation of the liquid crystals quickly, which led to the formation of the isotropic phase. As shown in the figures, the response time of the latter was much faster than that of the former.

The stability and reliability of the N–I phase transition of the homopolymer **P-10** was evaluated with a repeated cycle of 365 nm UV irradiation and then heated at 130°C. The results are summarized in Figure 8. After repeating the recycle phase transition nine times, no significant decay of the response and transmittance was seen. When a black sheet was attached behind the polymer film, as shown in Figure 9(a,b), image recording of the **P-10** films could be achieved after UV irradiation through a mask with pictures. The polymer film was irradiated around 60°C and then quenched to 25°C. The UV irradiated area was changed from an opaque glassy state to a clear isotropic phase, which led to the appearance of the black images.

CONCLUSIONS

A series of liquid-crystalline homopolymers and copolymers having azobenzene segments were synthesized. The molecular weights, phase-transition temperatures, and thermal properties of the polymers were evaluated. The UV–vis spectra of the polymers decreased around 355 nm with increasing UV irradiation. UV irradiation caused the formation of the bended structure of the Z-form azobenzene derivatives. Stronger intermolecular forces at the glassy state of polymers decreased the response of the UV-in-

duced isomerization. The excellent stability, reliability, and image recording characteristics of the polymer films prepared in this investigation were all evaluated.

The authors would like to thank the National Science Council (NSC) of the Republic of China (Taiwan) for financially supporting this research under Contract No. NSC 93-2216-E006-001.

References

1. Ikeda, T.; Horiuchi, S.; Karanjit, D. B.; Kurihara, S.; Tazuke, S. Macromolecules 1990, 23, 36.
2. Sasaki, T.; Ikeda, T.; Ichimura, K. Macromolecules 1992, 25, 3807.
3. Ikeda, T.; Tsutsumi, O. Science 1995, 268, 1873.
4. Shisido, A.; Tsutsumi, O.; Kanazawa, A.; Shiono, T.; Ikeda, T.; Tamai, N. J Phys Chem B 1997, 101, 2806.
5. Kurihara, S.; Sakamoto, A.; Nonaka, T. Macromolecules 1998, 31, 4648.
6. Tsutsumi, O.; Shiono, T.; Ikeda, T.; Galli, G. J Phys Chem B 1997, 101, 1332.
7. Tsutsumi, O.; Kanazawa, A.; Shiono, T.; Ikeda, T.; Park, L.-S. Phys Chem Chem Phys 1999, 1, 4219.
8. Shishido, A.; Tsutsumi, O.; Kanazawa, A.; Shiono, T.; Ikeda, T.; Tamai, N. J Am Chem Soc 1997, 119, 7791.
9. Lee, H.-K.; Kanazawa, A.; Shiono, T.; Ikeda, T.; Fujisawa, T.; Aizawa, M.; Lee, B. J Appl Phys 1999, 86, 5927.
10. Sackmann, E. J Am Chem Soc 1971, 93, 7088.
11. Lee, H.-K.; Doi, K.; Harada, H.; Tsutsumi, O.; Kanazawa, A.; Shiona, T.; Ikeda, T. J Phys Chem 2000, 104, 7023.
12. Kurihara, S.; Nomiyama, S.; Nonaka, T. Chem Mater 2000, 12, 9.
13. Kurihara, S.; Nomiyama, S.; Nonaka, T. Chem Mater 2001, 13, 1992.
14. Ruslim, C.; Ichimura, K. Adv Mater 2001, 13, 37.
15. Ruslim, C.; Ichimura, K. Adv Mater 2001, 13, 641.
16. Angeloni, A. S.; Caretti, D.; Carlini, C. Liq Cryst 1989, 4, 513.
17. Natansohn, A.; Rochon, P. Chem Rev 2002, 102, 4139.
18. Ikeda, T.; Horiuchi, S.; Karanjit, D. B.; Kurihara, S.; Tazuke, S. Macromolecules 1990, 23, 36.
19. Matczyszyn, K.; Bartkiewicz, S.; Sahraoui, B. Opt Mater 2002, 20, 57.
20. Kurihara, S.; Yoneyama, D.; Ogata, T.; Nonaka, T. J Appl Polym Sci 2003, 89, 943.
21. Weisner, U.; Reynolds, N.; Boeffel, C.; Spiess, H. W. Makromol Chem Rapid Commun 1991, 12, 457.
22. Weisner, U.; Reynolds, N.; Boeffel, C.; Spiess, H. W. Liq Cryst 1992, 11, 251.
23. Meng, X.; Natansohn, A.; Barrett, C.; Rochon, P. Macromolecules 1996, 29, 946.
24. Wu, S.; Yao, S.; She, W.; Luo, D.; Wang, H. J Mater Sci 2003, 38, 401.
25. Kurihara, S.; Sakamoto, S.; Nonaka, T. Macromolecules 1998, 31, 4648.
26. Liu, J. H.; Hung, H. J.; Wu, D. S.; Hong, S. M.; Fu, Y. G. J Appl Polym Sci 2005, 98, 88.
27. Liu, J. H.; Wu, D. S.; Tseng, K. Y. Macromol Chem Phys 2004, 205, 2205.
28. Liu, J. H.; Hung, H. J. Liq Cryst 2005, 32, 133.
29. Liu, J. H.; Yang, P. C. Liq Cryst 2005, 32, 539.
30. Liu, J. H.; Hsieh, C. D.; Tseng, C. C. J Appl Polym Sci 2005, 96, 1505.